Pergamon

Int. J. Heat Mass Transfer. Vol. 38, No. 15, pp. 2743–2748, 1995

0017-9310/95 $9.50+0.00

0017-9310(95)00047-X

Spectral collocation methods for one-dimensional phase-change problems

ROBERT SPALL

Department of Mechanical Engineering, EGCB 212, University of South Alabama, Mobile, AL 36688, U.S.A.

(*Received* 29 *July* 1994 *and in final form* 12 *January* 1995)

Abstract—Single and multi-domain spectral collocation methods utilizing Chebyshev polynomials were employed to obtain highly accurate solutions to one-dimensional phase-change problems. The Landau transformation was imposed to fix the position of the moving boundary. Spatial derivatives were approximated using both spectral and finite-difference representations. Solutions to the resulting ordinary differential equations in time were obtained using the Gear and Adams predictor-corrector algorithms as implemented within the Mathematica programming environment. For test problems in which exact solutions are available, results for the spectral representations compared favorably with solutions obtained using second-order accurate finite-difference approximations.

INTRODUCTION

The transient phase change or Stefan problem considered here involves the tracking of a sharp moving boundary, separating liquid and solid phases of a pure substance. Within each of the phases the heat transfer process is governed primarily by conduction. However, because of the nonlinearity of the interface condition, exact solutions are limited to a small number of idealized cases (cf. ref. [1]). Thus, numerical solution procedures are often employed. Most previous numerical works involve discretizations of the governing equations using either finite-difference or finite-element methods. These methods are generally implemented under the categories of (a) fixed grid methods [2]; (b) variable grid methods [3, 4]; (c) enthalpy methods [5, 6]; (d) front-fixing methods [2, 7]. For a comprehensive review, the reader is referred to the extensive work of Crank [8].

Spectral representations have recently become fashionable in the solution of fluid mechanics problems such as direct numerical simulations of turbulence and boundary-layer linear stability calculations (cf. ref. [9]). Based upon the successes for those difficult problems, it was decided to investigate the suitability of spectral methods for obtaining highly accurate solutions to phase-change problems. Compared with finite-difference and finite-element methods, relatively few grid points are needed for spectral discretizations (because of the global nature of the interpolating functions). This effectively renders fixed and variable grid methods impractical. Large gradients in the enthalpy function at the moving boundary also render enthalpy methods somewhat undesirable, at least for problems in which the phase change takes place at a fixed temperature. However, spectral collocation methods utilizing Chebyshev polynomials may readily be applied to front-fixing methods, and this is the approach taken here. This approach also provides for highly accurate calculations of the temperature gradients at the liquid/solid interface, hence the interface velocity and position is accurately computed.

In order better to assess the accuracy of the methods, test problems with analytical solutions have been chosen. More specifically, both one- and two-phase one-dimensional melting problems in a semi-infinite medium with constant material properties are considered (although the thermal diffusivity may vary between the liquid and solid phases). These test problems are solved numerically utilizing single- and multi-domain spectral representations. The approach within the category of front-fixing methods that is employed utilizes the Landau coordinate transformation and method of lines (MOL) (c.f. ref. [7]). The MOL involves the solution of a system of ordinary differential equations in time. In the present work, the set of ODEs is solved using either the Gear method (for stiff sets of equations) or the Adams predictor-corrector method within the Mathematica [10] programming environment. Results are compared with exact solutions, and with solutions obtained using second-order accurate finite-difference approximations (for the spatial derivatives).

GOVERNING EQUATIONS

The following linear heat conduction equation with constant coefficients governs the temperature distribution in each of the liquid ($i = 1$) and solid ($i = 2$) phases:

$$\frac{\partial u_i}{\partial t} - \alpha_i \frac{\partial^2 u_i}{\partial x^2} = 0, \quad t > 0. \tag{1}$$

NOMENCLATURE

E	elements of derivative matrix
F	elements of derivative matrix in physical domain
G	elements of second derivative matrix
H	elements of second derivative matrix in physical domain
k	thermal conductivity
l	domain length and length scale
$N1$	order of Chebyshev polynomials in zone I; number of grid points in finite-difference scheme
$N2$	order of Chebyshev polynomials in zone II; number of grid points in finite-difference scheme
s	front location
S	dimensionless front location s/l
St_1	Stefan number, zone I $(= C_1(u_L - u_m)/\chi)$
St_2	Stefan number, zone II $(= C_2(u_m - u_2)/\chi)$
t	time
u	temperature
x	Cartesian coordinate
$\hat{x}$	$(= x/l)$.

Greek symbols

α	thermal diffusivity
ε	Chebyshev variable
θ^{I}	dimensionless temperature in zone I $(= u - u_m/u_L - u_m)$
θ^{II}	dimensionless temperature in zone II $(= u - u_m/u_m - u_2)$
λ	interpolant for Chebyshev scheme
ξ	transformed coordinate
ρ	density
τ	dimensionless time $(= \alpha_1 t/l^2)$
υ	ratio of specific heats $(= \sqrt{\alpha_1/\alpha_2})$
ϕ	Chebyshev polynomial
χ	latent heat
$\tilde{\omega}$	scaling factor.

Superscripts

I	zone one (liquid phase)
II	zone two (solid phase).

Subscripts

j	index
L	$x = 0$ (left face)
m	melt temperature
1	zone one (liquid phase)
2	zone two (solid phase).

In the liquid phase $0 \leqslant x \leqslant s(t)$ and in the solid phase $s(t) \leqslant x \leqslant 1$ where $s(t)$ denotes the location of the moving boundary. An additional equation (resulting from an interface energy balance) for $s(t)$ is given as:

$$k_2 \frac{\partial u_2}{\partial x} - k_1 \frac{\partial u_1}{\partial x} = \rho\chi \frac{\mathrm{d}s}{\mathrm{d}t}, \quad \text{at } x = s(t) \quad t > 0. \tag{2}$$

In addition, at the interface $u_1 = u_2 = u_m$. The location of the moving boundary may be fixed through the Landau coordinate transformation [11]:

$$\xi_1 = \frac{x}{s(t)} \quad 0 \leqslant x \leqslant s(t) \tag{3a}$$

$$\xi_2 = \frac{x - l}{s(t) - l} \quad s(t) \leqslant x \leqslant l. \tag{3b}$$

This fixes the moving boundary so that at $x = s(t) \rightarrow \xi_1 = \xi_2 = 1$. Upon application of the coordinate transformation, and the introduction of dimensionless length, time and temperature variables, the appropriate form of the governing equations becomes (where for later convenience, superscripts I and II have been introduced, and are analogous to subscripts 1 and 2):

$$\frac{\partial \theta^{\mathrm{I}}}{\partial \tau} = \frac{1}{S^2} \frac{\partial^2 \theta^{\mathrm{I}}}{\partial \xi_1^2} + \left(\frac{\xi_1}{S} \frac{\mathrm{d}S}{\mathrm{d}\tau}\right) \frac{\partial \theta^{\mathrm{I}}}{\partial \xi_1} \quad \text{(liquid phase)} \tag{4a}$$

$$\frac{\partial \theta^{\mathrm{II}}}{\partial \tau} = \frac{1}{\upsilon^2 (S-1)^2} \frac{\partial^2 \theta^{\mathrm{II}}}{\partial \xi_2^2} + \left(\frac{\xi_2}{(S-1)} \frac{\mathrm{d}S}{\mathrm{d}\tau}\right) \frac{\partial \theta^{\mathrm{II}}}{\partial \xi_2} \quad \text{(solid phase)} \tag{4b}$$

$$\frac{\mathrm{d}S}{\mathrm{d}\tau} = \frac{St_2}{\upsilon^2 (S-1)} \frac{\partial \theta^{\mathrm{II}}}{\partial \xi_2} - \frac{St_1}{S} \frac{\partial \theta^{\mathrm{I}}}{\partial \xi_1} \quad \text{(interface).} \tag{4c}$$

The interface boundary condition becomes $\theta^{\mathrm{I}}(1, \tau) = \theta^{\mathrm{II}}(1, \tau) = 0$. In addition, $\theta^{\mathrm{I}}(0, \tau) = 1$ and $\theta^{\mathrm{II}}(0, \tau) = f(\tau)$. (For the cases to be calculated, the temperature on the left face is fixed, and the back-face temperature is defined as a function of time.)

NUMERICAL METHOD

Spectral methods are characterized by an expansion of the solution in terms of global basis functions. In the present case, since the temperature distribution is not periodic, Chebyshev polynomials have been chosen as the basic functions. Chebyshev polynomials exhibit rapid convergence rate with increasing numbers of terms, and also cluster the collocation points

near the boundaries [12]. One additional benefit is that, unlike higher order finite-difference methods, accurate treatments of derivative boundary conditions are easily implemented.

The Nth order polynomials P_N are defined on the interval $-1 \leqslant \varepsilon \leqslant 1$ and may be written as [12]:

$$\phi(\varepsilon) = \sum_{k=0}^{N} \lambda_k(\varepsilon)\phi(\varepsilon_k) \tag{5}$$

where the interpolant λ_k is given as:

$$\lambda_k(\varepsilon) = \left(\frac{1-\varepsilon_k^2}{\varepsilon-\varepsilon_k}\right)\frac{P'_N(\varepsilon)}{N^2 c_k}(-1)^{k+1}. \tag{6}$$

Here $c_0 = c_N = 2$ and $c_k = 1$, $0 < k < N$.
The collocation points ε_j are the extrema of P_N and are given as:

$$\varepsilon_j = \cos\left(\frac{\pi j}{N}\right), \quad j = 0, 1, \ldots N. \tag{7}$$

The first and second derivatives may then be written in the computational domain as [12]:

$$\left.\frac{\mathrm{d}\phi}{\mathrm{d}\varepsilon}\right|_j = \sum_{k=0}^{N} E_{jk}\phi_k \tag{8a}$$

and

$$\left.\frac{\mathrm{d}^2\phi}{\mathrm{d}\varepsilon^2}\right|_j = \sum_{k=0}^{N} G_{jk}\phi_k \tag{8b}$$

where,

$$E_{jk} = \frac{c_j}{c_k}\frac{(-1)^{k+j}}{\varepsilon_j-\varepsilon_k}, \quad j \neq k \tag{8c}$$

$$E_{jj} = -\frac{\varepsilon_j}{2(1-\varepsilon_j^2)} \tag{8d}$$

$$E_{00} = \frac{2N^2+1}{6} = -E_{NN} \tag{8e}$$

$$G_{jk} = E_{jm}E_{mk}. \tag{8f}$$

Since the physical domain may not range from $(-1, 1)$ a scaling factor between the physical and computational domains is defined as:

$$\bar{\omega}_j = \left.\frac{\partial\varepsilon}{\partial\xi}\right|_j \quad j = 0, 1, \ldots N. \tag{9}$$

The first and second derivative matrices in the physical domains are then written as $F_{jk} = \bar{\omega}E_{jk}$ and $H_{jk} = F_{jm}F_{mk}$ respectively.

The following discussion concerns a two-phase moving boundary problem. (The procedure for a single-phase problem is easily inferred from the discussion.) The physical domain is first divided into two domains, domain I, corresponding to the region in which the liquid phase exists, and domain II, corresponding to the region of the solid phase. Since the physical range in this problem is (0, 1) (within each domain) transformations between the computational and physical domains are defined as:

$$\varepsilon = 1-2\xi \quad \text{(domain I)} \tag{10a}$$

$$\varepsilon = 2\xi-1 \quad \text{(domain II)}. \tag{10b}$$

Equations (4a) and (4b) are then written in terms of truncated Chebyshev expansions at the collocation points in domains I and II respectively, where the collocation points are given as:

$$\varepsilon_j = \cos\left(\frac{\pi j}{N1}\right) \quad \text{(domain I; } j = 0, 1, \ldots N1\text{)} \tag{11a}$$

$$\varepsilon_j = \cos\left(\frac{\pi j}{N2}\right) \quad \text{(domain II; } j = 0, 1, \ldots N2\text{)}. \tag{11b}$$

The interface equation is, of course, also expressed in terms of the Chebyshev expansions. The resulting spectral representations of equations (4a)–(4c) are given as:

$$\frac{\mathrm{d}\theta_j^{\mathrm{I}}}{\mathrm{d}\tau} = \frac{1}{S^2}\sum_{k=0}^{N1} H_{jk}^{\mathrm{I}}\theta_k^{\mathrm{I}} + \frac{1-\varepsilon_1}{2}\frac{1}{S}\frac{\mathrm{d}S}{\mathrm{d}\tau}\sum_{k=0}^{N1} F_{jk}^{\mathrm{I}}\theta_k^{\mathrm{I}}$$

$$j = 1, 2, \ldots N1-1 \tag{12a}$$

$$\frac{\mathrm{d}\theta_j^{\mathrm{II}}}{\mathrm{d}\tau} = \frac{1}{v^2(S-1)^2}\sum_{k=0}^{N2} H_{jk}^{\mathrm{II}}\theta_k^{\mathrm{II}} + \frac{1+\varepsilon_2}{2}\frac{1}{(S-1)}\frac{\mathrm{d}S}{\mathrm{d}\tau}$$

$$\times \sum_{k=0}^{N2} F_{jk}^{\mathrm{II}}\theta_k^{\mathrm{II}} \quad j = 1, 2, \ldots N2-1 \tag{12b}$$

$$\frac{\mathrm{d}S}{\mathrm{d}\tau} = \frac{St_2}{v^2(S-1)}\sum_{k=0}^{N2} F_{0k}^{\mathrm{II}}\theta_k^{\mathrm{II}} - \frac{St_1}{S}\sum_{k=0}^{N1} F_{N1k}^{\mathrm{I}}\theta_k^{\mathrm{I}}. \tag{12c}$$

The resulting set of $N1+N2-1$ ordinary differential equations are solved utilizing a variable time step ODE solver provided within the Mathematica [10] programming language. The routine **NDSolve** uses an Adams predictor–corrector method for non-stiff differential equations and the Gear method for stiff equations. The routine switches between the two methods using heuristics based on the adaptive step size. The algorithms and the heuristics for switching are described in Hindmarsh [13] and Petzold [14].

Solutions have also been obtained in which the spatial derivatives were approximated using second-order accurate finite-difference expressions. The discretized form of these equations may be found in the work of Furzeland [7]. The solutions to this resulting system of ODEs are also obtained using **NDSolve**. (Note that when the finite-difference approximations are discussed in the Results section, N refers to the number of grid points. When spectral representations are discussed, N represents a quantity one less than the number of collocation points.)

Since the equations are singular at $\tau = 0$, the functional evaluations required within **NDSolve** (at $\tau = 0$) cannot be performed. Hence, some alternative means of starting the solution must be used. One method is to employ a first-order accurate implicit time dis-

cretization for equations (12a)–(12c) for the first time step. This then provides NDSolve with a set of initial conditions and a non-zero value of S. NDSolve may then be employed to advance the solution in time. However, since the purpose of this paper is to provide comparisons between spectral and finite-difference spatial difference schemes, the exact solution at $\tau = 10^{-8}$ is used to provide the initial conditions. This removes any uncertainty in the results caused by the initial conditions that might be provided by the implicit time discretization. In addition, for the two-phase problem, the exact temperature (as a function of time) was specified at the back face ($x = l$). This again was for the purpose of removing uncertainty due to the specification approximate boundary conditions.

RESULTS

Results are first presented for a single-phase melting problem in a semi-infinite medium. Comparisons with results obtained using second-order accurate finite-difference approximations are presented (in terms of front location and CPU times). Results for the CPU times include only the time to solve the respective initial value problem (i.e. excluding the time to set up the ODEs, which is minimal) and were obtained using the Mathematica Timing routine. In addition, the PrecisionGoal setting within the Mathematica routine NDSolve was set to 10 digits. (PrecisionGoal is an option to NDSolve which specifies how many digits of precision, in terms of relative error, should be sought in the final result.) Of course, changing the precision to which the relative error of the solutions is computed will affect the CPU time. In fact, lower levels of precision could have been specified without affecting the final absolute error (due to the spatial discretizations) in the front location for both the finite-difference and spectral methods in cases where the spatial discretizations were coarse. However, for consistency, a value of 10 digits was used throughout.

Figure 1 shows results in terms of front location for a Stefan number of 1 for both spectral collocation and second-order-accurate finite-difference approximations at time $\tau = 0.25$. CPU times (in seconds, on a Sun SPARC10 workstation) are also shown. The rapid convergence rates of the spectral method are clearly indicated, as is the second-order convergence of the finite-difference approximation. For the spectral method at a Stefan number of 1, absolute errors of order 10^{-8} are achieved with CPU times of approximately 13 s (the exact solution is given as $S = 0.62188136$, cf. ref. [1]). As a measure of efficiency, it is noted that for equal CPU time, errors for the spectral method are up to four orders of magnitude smaller than for the finite-difference method. (Of course, if the number of grid points is held constant, more CPU time is required by the spectral method than the finite-difference method.) Although the results for the one-phase case are very impressive, from a practical point of view, the performance of the spectral method in the two-phase case is more relevant.

Numerical experiments revealed that, for the two-phase Stephan problem, the accuracy was governed primarily by the number of grid points in domain II. Shown in Fig. 2(a) is the absolute error of the interface location for a two-phase problem as a function of $N2$ for $St_1 = St_2 = 1$ at $\tau = 0.075$ (the exact solution is $S = 0.20690756$, cf. ref. [1]). The number of grid points in domain I was set to 7 for the spectral scheme and 10 for the finite-difference scheme (recall that the number of grid or collocation points for the spectral scheme equals $N+1$, thus $N1 = 6$). Increasing the number of points beyond these values had little effect on the resultant accuracy. The spectral calculations were run on two different grids, one as defined by equations (10a) and (10b) and another that employed an algebraic stretching function designed to cluster points towards the moving boundary in domain II. That stretching was defined as $\xi = a(1+\varepsilon)/(b-\varepsilon)$, where $b = 1+2a$ and $a = \hat{\xi}/(1-2\hat{\xi})$. Here $\hat{\xi}$ is the location corresponding to $\varepsilon = 0$. A value of $\hat{\xi} = 0.75$

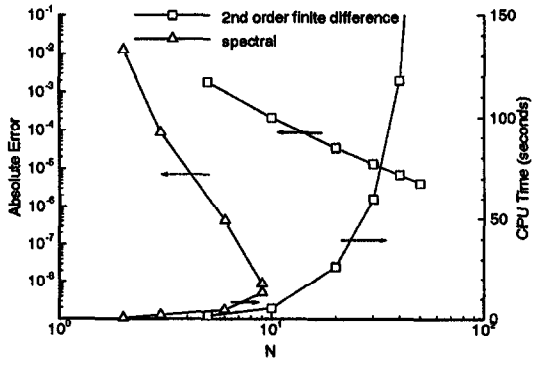

Fig. 1. Comparison of absolute error in the computed location of the moving boundary (and the associated CPU time) between spectral collocation and finite-difference schemes for the single-phase problem ($St = 1$) as a function of the number of grid points.

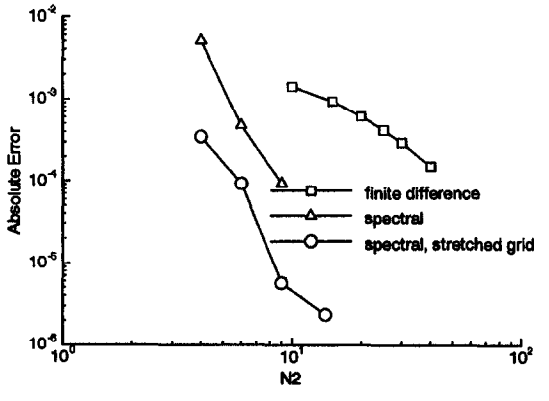

Fig. 2. Absolute error in the computed location of the moving boundary as a function of number of grid points for the two-phase problem ($St_1 = St_2 = 1$).

was chosen. The effectiveness of this grid clustering is quite evident, providing roughly an order of magnitude decrease in the absolute error with respect to the distribution defined by equations (10a) and (10b). (Of course, clustering should also improve the accuracy of the finite-difference scheme, but since the emphasis is on spectral representations, this exercise was not performed.) In summary, for both the spectral and finite-difference schemes, the accuracies achieved for the two-phase case are less than achieved for the single-phase case. However, relative to the finite-difference scheme, the spectral scheme still provides a much higher convergence rate.

The decrease in accuracy is due to the existence of extremely large temperature gradients at the moving boundary (in domain II) for a small time. Accurate resolution of these gradients (or the heat flux) is essential if the numerical scheme is to track the front movement accurately. Figure 3(a) shows a comparison of the relative error in the temperature gradient at the front location in domain II for the spectral calculations (without stretching) for $N2 = 4$ and 9 (corresponding to 5 and 10 collocation points respectively). The rapid convergence of the first (spatial) derivative is quite apparent. With $N2 = 9$ the relative error is quite small for $\tau > 0.01$. This time level corresponds to an interface location $S \approx 0.076$. In addition, the exact interface location (to 3 significant digits) at $\tau = 0.075$ is $S = 0.207$. Hence, although large errors in the temperature gradient are restricted to small time, the front velocities are large, and the front has already traversed a significant portion of the domain. However, with $N2 = 4$, significant errors exist over the entire range $0 \leqslant \tau \leqslant 0.075$, and it is understandable that for this case the errors in terms of interface location are relatively large. It is further noted that when the numerical calculations were initiated at $\tau = 0.01$ (with exact initial conditions) the large gradients at the front (with the associated errors) were eliminated, and convergence rates comparable to the single-phase problem were achieved.

Shown in Fig. 3(b) are similar calculations for the finite-difference scheme with $N2 = 10$ and 20. Relative errors are significantly larger than for the spectral calculations (with $N2 = 9$) and the superior convergence rate of the spectral scheme is clearly revealed. (It is noted that errors in the temperature gradient at the moving boundary in domain I are much smaller than those in domain II for both spectral and finite-difference schemes and do not significantly affect the results, thus they are not presented.)

Absolute errors in the (dimensionless) temperature profiles are next examined in Figs. 4(a) and (b) at $\tau = 0.075$. Figure 4(a) shows results for the spectral scheme for $N2 = 4$, 9 and 14 (with $N1 = 6$). The rapid rate of convergence is demonstrated, with absolute errors decreasing by 2–3 orders of magnitude for a threefold increase in the number of collocation points. In contrast, the convergence rate for the finite-difference calculations as shown in Fig. 4(b) (for $N2 = 10$, 20, 30 and 40, $N1 = 10$) is much less impressive,

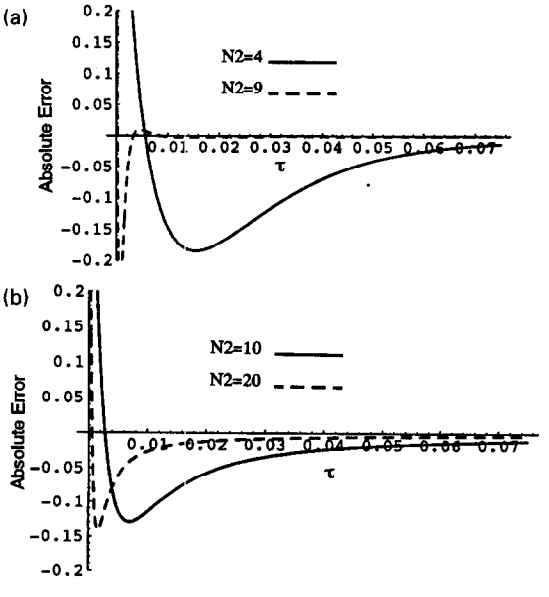

Fig. 3. Absolute error of first derivative of temperature ($\partial\theta^{II}/\partial\hat{x}$) in zone II at the location of the moving boundary interface: (a) spectral collocation method; (b) finite-difference method.

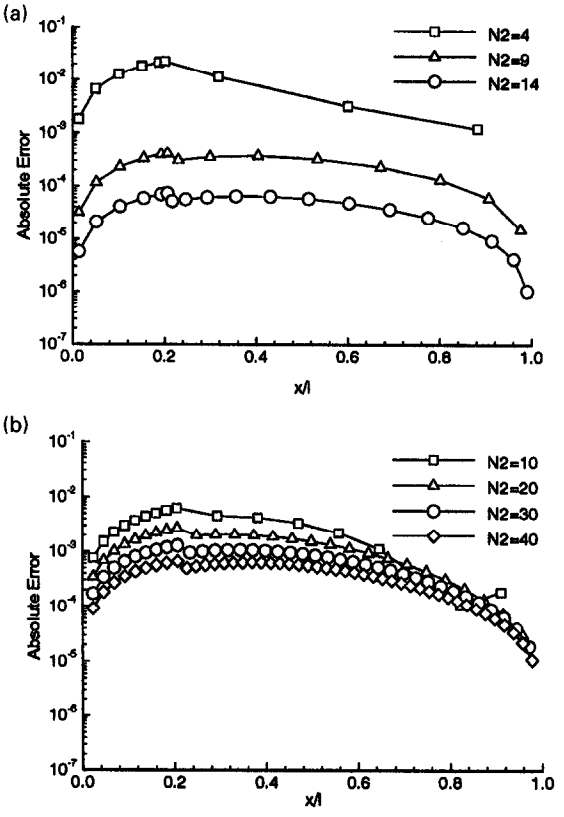

Fig. 4. Absolute errors in temperature as a function of $\hat{x}$ and $N2$: (a) spectral collocation method; (b) finite-difference method.

although maximum absolute errors using 40 grid points are only about 1 order of magnitude larger than obtained with the spectral scheme using 15 collocation points. Although not shown, results for the spectral scheme employing the previously described grid clustering improved the accuracy, with maximum absolute errors on the order of 10^{-5} to 10^{-6} when 15 collocation points were employed.

SUMMARY

Spectral collocation methods employing Chebyshev polynomials provide an accurate and efficient means for computing solutions to one-dimensional phase-change problems within the context of front-fixing methods. Convergence rates (in terms of the front location and temperature profiles) much higher than those obtained using second-order accurate finite-difference methods were achieved. A source of inaccuracy for both spectral and finite-difference schemes concerns the calculation of the temperature gradient at the moving boundary in the solid phase at early time levels. Although the accuracy of spectral methods is known to decrease in regions of large gradients, the computed results for the temperature gradient in the solid region at the moving boundary compared favorably with those of the finite-difference scheme. The implementation of grid clustering towards the moving boundary in the solid region was also found to reduce significantly the levels of error throughout the domain.

As a result of the high accuracy achieved with the spectral methods, the program will, in the future, be extended to include variable properties, and will be utilized in the calculation of laser–solid interactions for applications involving laser surface treatments (where the one-dimensional approximation is appropriate). The author found the Mathematica programming environment to be quite useful, and as a result, the extended code will be implemented as a Mathematica package and made available to interested users.

Acknowledgments—The author would like to acknowledge the NASA EPSCOR program for supporting this work.

REFERENCES

1. V. Alexiades and A. D. Solomon, Mathematical modeling of melting and freezing processes, Hemisphere, Washington, DC (1993).
2. J. Crank, Two methods for the numerical solution of moving-boundary problems in diffusion and heat flow, *J. Mech. Appl. Math.* **10,** 220–231 (1957).
3. R. S. Gupta, Moving grid method without interpolations, *Comp. Meth. Appl. Mech. Engng* **4,** 143–152 (1974).
4. R. S. Gupta and D. Kumar, Variable time step methods for one-dimensional Stefan problem with mixed boundary condition, *Int. J. Heat Mass Transfer* **24,** 251–259 (1981).
5. V. Voller and M. Cross, Accurate solutions of moving boundary problems using the enthalpy method, *Int. J. Heat Mass Transfer* **24,** 545–556 (1981).
6. V. R. Voller and C. R. Swaminathan, Fixed grid techniques for phase change problems: a review, *Int. J. Numer. Meth. Engng* **30,** 875–898 (1990).
7. R. M. Furzeland, A comparative study of numerical methods for moving boundary problems, *J. Inst. Math. Appl.* **26,** 411–429 (1980).
8. J. Crank, *Free and Moving Boundary Problems*. Clarendon Press, Oxford (1984).
9. M. Y. Hussaini and T. A. Zang, Spectral methods in fluid dynamics, *Ann. Rev. Fluid Mech.* **19,** 339–367 (1987).
10. S. Wolfram, *Mathematica: A System for Doing Mathematics by Computer*. Addison-Wesley, New York (1992).
11. H. G. Landau, Heat conduction in a melting solid, *Quart. Appl. Math.* **8,** 81–94 (1950).
12. D. Gottlieb, M. Y. Hussaini and S. A. Orszag, Theory and applications of spectral methods. In *Spectral Methods for Partial Differential Equations* (Edited by R. G. Voigt, D. Gottlieb and M. Y. Hussaini), SIAM-CBMS, Philadelphia (1984).
13. A. C. Hindmarsh, ODEPACK: a systemized collection of ODE solvers. In *Scientific Computing* (Edited by R. S. Stepleman *et al.*), pp. 55–64. North-Holland, Amsterdam (1983).
14. L. R. Petzold, Automatic selection of methods for solving stiff and nonstiff systems of ordinary differential equations, *SIAM J. Sci. Statistical Computing* **4,** 136–148 (1983).